CBIS'24
XX Congresso Brasileiro de Informática em Saúde
08/10 a 11/10 de 2024 - Belo Horizonte/MG - Brasil

CovNet-UFCSPA: assisting in the diagnosis of pneumonia by coronavirus

CovNet-UFCSPA: auxiliando no diagnóstico de pneumonia por coronavírus

CovNet-UFCSPA: ayudando en el diagnóstico de neumonía por coronavirus

Nouara Cândida Xavier[1], Rochelle Lykawka[2], Alexandre Bacelar[2], Tiago Severo Garcia[3], Thatiane Alves Pianoschi Alva[4], Mirko Salomón Alva Sánchez[4] , Carla Diniz Lopes Becker[4]

1 M.Sc., Federal University of Health Sciences of Porto Alegre – UFCSPA, Porto Alegre (RS), Brazil.
2 M.Sc., Hospital de Clínicas de Porto Alegre, Porto Alegre (RS), Brazil, Brazil.
3 Ph.D, Hospital de Clínicas de Porto Alegre, Porto Alegre (RS), Brazil, Brazil.
4 Ph.D., Federal University of Health Sciences of Porto Alegre – UFCSPA, DECESA, Porto Alegre (RS), Brazil.

Autor correspondente: Nouara Cândida Xavier
E-mail: nouaracandida@gmail.com
Links: https://github.com/nouxavier/CovNet-UFCSPA

Abstract

Objective: This study introduces the CovNet-UFCSPA architecture, which incorporates pre-processing data from clinical images (X-rays) and deep learning algorithms. **Method:** A total of 24,235 images were used for training, validation, and testing of the model, identifying areas in the X-rays that influence the model's decision. **Result:** The architecture achieved a recall of 99% in classifying X-rays from patients at the Hospital de Clínicas de Porto Alegre (HCPA). The application of the CLAHE technique improved the region of interest in the X-rays, reducing the false negative rate from 187 to 9. **Conclusion:** Compared with Resnet50 V2 and Inception V3 architectures, CovNet-UFCSPA demonstrated superiority in false negative rates, true positives, and recall.

Keywords: CNN; Deep Learning; COVID-19

Resumo

Objetivo: O presente estudo introduz a arquitetura CovNet-UFCSPA, que incorpora dados de pré-processamento de imagens clínicas (raio-X) e algoritmos de aprendizado profundo. **Método:** Utilizou-se um total de 24.235 imagens para treinamento, validação e teste do modelo, identificando áreas nos raios X que influenciam a decisão do modelo. **Resultado:** A arquitetura atingiu um recall de 99% na classificação de raios X de pacientes do Hospital de Clínicas de Porto Alegre (HCPA). A aplicação da técnica CLAHE melhorou a região de interesse do raio-X, reduzindo a taxa de falsos negativos de 187 para 9. **Conclusão:** Comparada com as arquiteturas Resnet50 V2 e Inception V3, a CovNet-UFCSPA demonstrou superioridade em taxas de falsos negativos, verdadeiros positivos e recall.

Palavras-chave: CNN; Aprendizado Profundo, COVID-19.

Resumen

Objetivo: Este estudio presenta la arquitectura CovNet-UFCSPA, que incorpora datos de preprocesamiento de imágenes clínicas (radiografías) y algoritmos de aprendizaje profundo. **Método:** Se utilizaron un total de 24,235 imágenes para el entrenamiento, validación y prueba del modelo, identificando áreas en las radiografías que influyen en la decisión del modelo. **Resultado:** La arquitectura alcanzó un recall del 99% en la clasificación de radiografías de pacientes del Hospital de Clínicas de Porto Alegre (HCPA). La aplicación de la técnica CLAHE mejoró la región de interés en las radiografías, reduciendo la tasa de falsos negativos de 187 a 9. **Conclusión:** En comparación con las arquitecturas Resnet50 V2 e Inception V3, CovNet-UFCSPA demostró superioridad en las tasas de falsos negativos, verdaderos positivos y recall.

Descriptores: CNN; Aprendizaje Profundo; COVID-19.

Introduction

Early diagnosis of COVID-19 has proven to be extremely efficient in reducing the risk of death for a patient and the risk of the disease progressing to a critical stage [1]. However, in places far from large centers, the capacity of the tests is generally limited, due to the lack of inputs, thus making it necessary to search for alternatives for detecting the disease. Therefore, seeking to combat and mitigate the effects of the pandemic, SARS-CoV-2 identification strategies, ranging from applying serological tests to testing by reverse transcription polymerase chain reaction (RT-PCR), surveillance of cases and analysis of computed tomography (CT) [2]. In Brazil, the most common exam to evaluate pulmonary illness is conventional X-Ray and in a few cases computerized tomography. However, Brazil has only one tomograph per 100,000 inhabitants, with geographic distribution concentrated in large centers since the proportion of X-ray equipment is four times greater [3].

Deep machine learning (DML) algorithms can aid in the diagnosis of certain pathologies, such as tuberculosis and lung cancer, using chest X-rays at a level comparable to radiologists [4]. Using DML with image pre-processing techniques proved highly accurate in detecting pneumonia [5]. As a result, several works seeking to optimize, accelerate and assist the screening of patients with COVID-19 are are under development using DML, such as Rajaraman and Antani (2020) [6] which, using DML, identifies patients with pneumonia induced by COVID-19 using X-rays weakly labeled thorax, similar techniques is present in the work of, [7], [8], and [9].

This project aims to create an architecture called CovNet-UFCSPA, using data from clinical images (X-ray), to identify possible patients with COVID-19 and patients without the pathology. This dataset has 817 images of patients diagnosed with COVID-19 and 721 images without COVID-19. In addition, this architecture will test its performance with the support of the Hospital da Clínicas de Porto Alegre (HCPA), where images of 1538 patients diagnosed with and without COVID-19 will be apply to CovNet-UFCSPA.

Materials

Data acquisition

The data acquisition process involved accessing datasets sourced from an integrative review [10], which contributed 22,697 images to our dataset. Additionally, data from the project "Application of an algorithm with artificial intelligence to aid in diagnosing COVID-19," registered on Plataforma Brasil under researcher Alexandre Bacelar, with CAAE 35219020.1.0000.5327, was utilized. This project was approved by the Research Ethics Committee (CEP) of the Hospital de Clínicas de Porto Alegre, Federal University of Rio Grande do Sul, under opinion number 4,508,683. Furthermore, we obtained 817 images of patients diagnosed with COVID-19 and 721 images of patients without COVID-19 to evaluate the performance of the proposed architecture.

Data pre-processing

The study on differentiating COVID-19 from non-COVID-19 cases in medical images employs a supervised learning approach, utilizing labels in a CSV file where each filename is linked to an image, and the label indicates whether it represents COVID-19 (1) or not (0). Radiographs from HCPA are manually clipped to focus solely on the thorax, eliminating non-essential parts caused by varying image positions. All images are resized to consistent dimensions using the OpenCV library, . Furthermore, Global Contrast Equalization (GCE) adjusts the histogram across images to even out gray levels based on the intensity values' probability distribution [11]. Additionally, Contrast Limited Adaptive Histogram Equalization (CLAHE) enhances the visibility of textures and contrasts [11] in COVID-19 patient images, significantly improving diagnostic clarity, in Figure 1 is example.

Heat Map

Deep Machine Learning (DML) algorithms are increasingly used in critical tasks such as medical diagnoses. To understand how these algorithms make decisions, heat map tracing is used to visualize the active areas in an image during task classification [13]. This technique highlights the parts of the image deemed significant by the algorithm, helping to debug the decision-making process of Convolutional Neural Networks (CNNs). Specifically, this method was applied to analyze x-rays in a study using the CovNet-UFCSPA model. In the test phase, a heatmap was used on an x-ray from the HCPA test set, where areas with more intense red indicate higher attention from the CNN, which successfully identified the image as indicative of COVID-19.

a) Original image b) Cropped image c) Resized image d) GCE image e) CLAHE image

Figure 1 – Pre-processing of an image of a patient with COVID-19 at HCPA.

Architecture

Convolutional Neural Networks

Convolutional Neural Networks (CNNs) are a well-established subset of Advanced Machine Perception (AMP) models widely utilized in medical fields, including radiology [14]. Their performance matches that of specialist radiologists and is utilized in various applications such as lesion detection, classification, image segmentation, and reconstruction. CNNs are composed of multiple layers: convolutional layers that use filters or kernels to extract and preserve essential features from images, pooling layers that reduce the data complexity and dimensionality from convolutions, thereby lowering the computational demand and the number of parameters, and fully connected layers where the extracted high-level features (feature maps) are transformed into a one-dimensional vector for the classification process [15]. A notable feature of CNNs is their ability to recognize the intended class of an image regardless of its orientation, and their capability to derive more abstract features as inputs move to deeper layers [16]. This research specifically employs convolutional neural networks due to these capabilities.

CovNet-UFCSPA

The CovNet-UFCSPA architecture, utilizing the Keras library, consists of multiple layers starting with an input shape of (224, 224, 3) and a 16-value filter. Convolutional layers use the relu activation function with progressively increasing filters from 32 up to 64. Max pooling of (2,2) is interleaved among layers. The design also includes GlobalAveragePooling2D, BatchNormalization, Dropout, and two Dense layers.

Pretrained Network

Using pre-trained networks consists of taking resources learned in a problem and using them in a new and similar problem. This technique brings benefits when the dataset is not large enough. This process is also applied to decrease the depth of the CNNs, since the more profound the CNNs, the higher their computational cost. This technique can be used in two ways: feature extraction and fine-tuning. In this work, the feature extraction technique is approached. For performance comparison, the ResNe50V2 and Inception V3 architectures.

Architecture Performance Analysis

For the quantitative analysis of the architecture, the following metrics were selected: accuracy, F1-Score, recall, precision, confusion matrix, and receiver operating characteristic curve (ROC) area. In addition, the true positive (TP), true negative (TN), false positive (FP), and false negative (FN) classifications will also be used for the confusion matrix compositions.

Hardware

The tests were carried out at Santos Dumont from the National Laboratory of Scientific Computing, in the Fast-track for COVID-19 SCALAC allocation program.

Methods

Data division

The data were divided into three parts for this experiment: training, validation, and testing. The experiment data are the images acquired in partnership with the HCPA. For the experiment, 22 697 images were used: 17 504 training images, where 7 504 were of patients with COVID-19. For validation, 4,376 x-rays were applied, 1,876 of which were from patients with COVID-19.

The test stage of the experiment was performed exclusively with HCPA patients; these images were acquired by the project "Application of an algorithm with artificial intelligence to aid in diagnosing COVID-19". In addition, this project made X-rays of patients with and without COVID-19 available. However, to evaluate the behavior of the network when receiving positive samples, experiment I and II were performed only with images of patients with COVID-19.

To train the model, the class_weight function from the sklearn library was applied since there is an imbalance between the classes in the training stage [17].

Experiment Methods I

This experiment seeks to identify the efficiency of the CovNet-UFCSPA architecture when tested on a dataset of Brazilian patients from the HCPA.

Procedures

Table 1 outlines the hyperparameters utilized in this study, employing the sklearn library's StratifiedKFold for cross-validation. The experiment involved preprocessing HCPA original images to assess different preprocessing effects, testing each model four times. Preprocessing methods included resizing all images (even the originals), clipping, GCE, and CLAHE. The model underwent training, validation, and testing across five folds, with each test conducted four times. Due to the test phase only including COVID-19 positive samples, precision measures like ROC Area, FP, and TN were not assessed.

Experiment Methods II

This experiment aims to analyze the performance of the CovNet-UFCSPA architecture when compared to other pre-trained models: Resnet50V2 and Inception V3. For the quantitative evaluation of this comparison, the following metrics will be used: accuracy, F-Score, recall, confusion matrix, FN TP, and test execution time. Precision measures and TP and TN rates will not be applied due to the dataset in this test step having only patients with COVID-19.

Procedures

Three jobs were executed at Santos Dumont, each focusing on training, validating, and testing a specific model using the same dataset mentioned previously. This dataset includes 817 images of COVID-19 diagnosed patients from HCPA hospital. The preprocessing steps for the test data mirror those in Experiment I. Table 1 provides detailed hyperparameter values and the execution times for each tested architecture.

Table 1: Informations experimentos I and II

Informations	Experiment I	Experiment II
Architecture	CovNet-UFCSPA	CovNet-UFCSPA/ ResNet 50 V2/ Inception V3
Batch Size	500	1500
Learning rate	0000.1	0000.1
Optimizer	Adam	Adam

Dropout	0.4	0.4
Loss	Binary crossentropy	Binary crossentropy
Epoch	500	250
Cross validation	StratifiedKFold with 5 folds	Not apply
Enviroment	Santos Dumont - 1 nó - 4 GPUs Tesla V100-SXM2-32GB	Dantos Dumont - 1 nó - 4 GPUs Tesla V100-SXM2-32GB
Pre-processing step time	Time to train the fold 1: 1 hour and 7 minutes Time to train the fold 2: 1 hour and 7 minutes Time to train the fold 3: 1 hour and 6 minutes Time to train the fold 4: 1 hour and 7 minutes Time to train the fold 5: 1 hour and 7 minutes	Time to train CovNet-UFCSPA: 1 hora e 7 minutos Time to train ResNet 50 V2: 1 hora e 20 minutos Time to train Inception V3: 1 hora e 15 minutos

Experiment III

The objective of this essay is to carry out an analysis of the behavior of the implemented networks. This test will run the following models: Resnet50V2, Inception V3, and CovNet-UFCSPA.For the quantitative evaluation of this test, the following metrics will be used: accuracy, F-Score, recall, confusion matrix, ROC curve, and test execution time. In addition, accuracy measures and FP and TN rates will be applied due to this dataset containing patients with and without COVID-19.

Procedures

Four jobs were submitted at Santos Dumont for this test, each job tested each model. Training and validation were not carried out in this test since the best result from previous tests was used. With that, a file with the extension H5 was loaded. This file saved all the model progress during the training stage.

The test stage consists of 817 images of patients diagnosed with COVID-19 and 721 images without COVID-19. All of these test images received a report from the HCPA. However, the H5 files used were tested and validated with 21,880 images, containing the weights with the best result obtained after experiment I and II.

Results

Experiment I: CovNet-UFCSPA architecture assisting in the diagnosis of COVID-19 in HCPA patients

The CovNet-UFCSPA architecture's performance is detailed in this section, focusing on accuracy and error metrics during the training and validation phases, illustrated in

Figures 2. The architecture demonstrated convergence across all five folds, indicating consistent learning and model improvement.

This particular trial focused exclusively on COVID-19 positive X-rays from HCPA patients, not including healthy chest X-rays, which means that metrics such as FP , TN (, and ROC curve area are not applicable or presented. The results of the architecture's performance across different preprocessing scenarios are summarized in Table 2. Specifically, Fold 1 using original images achieved an 86% recall rate, correctly diagnosing 706 out of 817 images. In contrast, the same fold using cropped images significantly improved recall to 98%, with 804 images correctly classified and only 13 misclassifications. This highlights a 12% improvement in recall due to focusing on key image areas through cropping.

Further comparisons between different preprocessing methods show that the use of GCE resulted in a decrease in recall compared to cropped images. However, applying CLAHE to Fold 1 led to a slight improvement over the cropped images, with a recall of 99%—806 out of 817 images were correctly diagnosed.

This enhanced recall with CLAHE application was consistent, as evidenced in Table 2, which shows a 5% increase in recall for Fold 2 compared to the cropped images. This indicates that specific preprocessing techniques, particularly CLAHE, can significantly influence the accuracy and reliability of the model in diagnosing COVID-19 from X-ray images.

Table 2: Results experiment I and II

Architecture	Fold	Recall	F-Score	Accuracy	TP	FN	FP	TN
CovNet-UFCSPA Original Images	Fold 1	86%	93%	86%	705	112	0	0
	Fold 2	77%	87%	77%	627	190	0	0
	Fold 3	79%	88%	79%	647	170	0	0
	Fold 4	81%	90%	81%	663	154	0	0
	Fold 5	81%	89%	81%	660	157	0	0
CovNet-UFCSPA Cropped Images	Fold 1	98%	99%	98%	804	13	0	0
	Fold 2	90%	95%	90%	733	84	0	0
	Fold 3	91%	95%	91%	740	77	0	0
	Fold 4	94%	97%	94%	769	48	0	0
	Fold 5	94%	97%	94%	764	53	0	0
CovNet-UFCSPA GCE Images	Fold 1	94%	97%	94%	768	49	0	0
	Fold 2	85%	92%	85%	692	125	0	0
	Fold 3	81%	90%	81%	665	152	0	0

	Fold 4	87%	93%	87%	709	108	0	0
	Fold 5	90%	90%	90%	733	84	0	0
CovNet-UFCSPA CLAHE Images	Fold 1	99%	99%	99%	806	11	0	0
	Fold 2	95%	97%	95%	777	40	0	0
	Fold 3	95%	98%	95%	780	37	0	0
	Fold 4	97%	98%	97%	789	28	0	0

Heatmap

The implementation of the heat map was applied to track which areas the CovNet-UFCSPA architecture took into account when classifying an image with or without COVID-19. The execution of this test was carried out at section 2.4.3. All 817 images were mapped. This section will discuss three cases, as presented in Table 3. This table presents the labeled class of each case; all selected cases were obtained from images of patients with COVID-19 at HCPA, and the other columns show the prediction value generated by the model, so the closer to 100%, the more certainty the model had when classifying, the image class, this value was called score.

The first case shows that when receiving the original image from HCPA, the model labeled the score at 45%, but when classifying a cropped image, the score is 94%. Images with contrast adjustment received a score of 91% for images that underwent the GCE process and 98% for images with CLAHE. The heatmap of the four images of the first case is presented in Figure 3. In the figure, the areas where the hue approaches red mean that the model understands it has greater relevance for the COVID-19 class. The areas of activation are depicted in Figure 3.

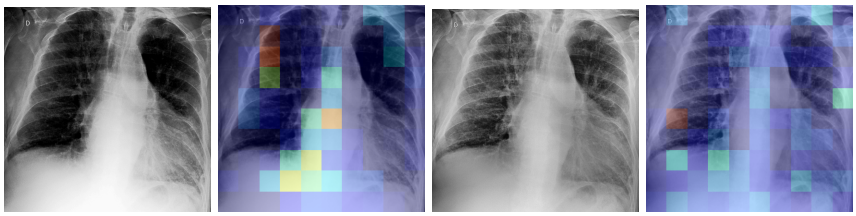

GCE CLAHE

Figure 3: Heatmap case I

Table 3: Data set

Informations	Class	Score originals	Score cropped	Score GCE	Score CLAHE
Case I	COVID-19	45%	94%	91%	98%
Case II	COVID-19	35%	86%	36%	98%
Case III	COVID-19	0%	0%	0%	0%

Experiment II: Comparative analysis of pre-trained networks with the CovNet-UFCSPA architecture

The table 4 presents the results of this test. When comparing the confusion matrix of the four test sets, the CLAHE technique again proved relevant for model performance, as the lowest NF rates are from this data set. The CovNet-UFCSPA architecture obtained the best TP and FN metrics in all four datasets. Then the Resnet50V2 model obtained the best results, except in the cropped image dataset, where Inception V3 had a lower FN rate in this case.

Recall is the metric that observes the network's performance about positive samples (with COVID-19) CovNet-UFCSPA showed the best result with a value of 99%, then Resnet50V2 with 97% and Inception V3 with 95% being all in the dataset with CLAHE. The CovNet-UFCSPA architecture boasts the shortest execution time at 1 hour and 7 minutes, attributed to its fewer convolutional layers. Although the ResNet50 V2 and Inception V3 models utilized the resource extraction technique from pre-trained networks, resulting in execution times comparable to CovNet-UFCSPA, they required distributed training when operating with a batch size of 1000. To facilitate this, the MirroredStrategy technique from TensorFlow was employed.

Experiment III: Identification of cases with and without COVID-19

In a trial using 1538 images, split between 817 COVID-19 positive and 721 COVID-19 negative cases, the CovNet-UFCSPA, ResNet50 V2, and Inception V3

architectures were tested. The CovNet-UFCSPA yielded 36 false negatives (FN) and 242 false positives (FP), translating to FN and FP rates of 2.34% and 15.7%, respectively. ResNet50 V2 recorded 63 FNs and 175 FPs, resulting in rates of 4.1% FN and 11.38% FP. Inception V3, the least effective, had 70 FNs and 407 FPs, with rates of 4.55% FN and 26.46% FP.

The application of the CLAHE preprocessing technique to all images in the dataset yielded mixed results. CovNet-UFCSPA achieved a 59% accuracy with a ROC area of 0.574, whereas ResNet50V2 showed better performance with 78% accuracy and a ROC area of 0.774. Inception V3 had the lowest scores, with 55% accuracy and a ROC area of 0.54. A subset of clipped data provided the second-best outcomes, with accuracies of 80% for CovNet-UFCSPA, 77% for ResNet50V2, and 65% for Inception V3.

Experiment II focused solely on COVID-19 positive images. Pre-processing with CLAHE reduced FNs significantly from 112 to 11 when using only COVID-19 positive images. However, applying CLAHE to a mixed dataset of COVID-19 positive and negative images led to a decrease in model reliability, with accuracies of 54% for both CovNet-UFCSPA and Inception V3, and 72% for ResNet50 V2. This drop in accuracy suggests that the varied image quality within the mixed dataset affected the models' performance.

Overall, the best performance was observed in the mixed dataset, with ResNet50 V2 achieving the highest accuracy of 85%, while CovNet-UFCSPA scored 82%. This marked a significant decrease from Experiment I, likely due to the smaller number of COVID-19 positive images, variation in patient demographics, and differences in image acquisition techniques affecting image quality.

Tabela 4: Table Results Experiment II and III

Dataset	Architecture	Prec.		Recall		F-Score		Accuracy		ROC		TP		FN		FP		TN	
		II	III	II	III	II	III	II	III	II	III	II	III	II	III	II	III	II	III
Original Images	CovNet-UFCSPA	NA	72%	77%	76%	87%	74%	77%	72%	NA	0,72	631	619	187	199	0	244	0	527
	ResNet50 V2	NA	70%	62%	51%	76%	59%	62%	64%	NA	0,641	506	417	312	401	0	176	0	595
	Inception V3	NA	59%	71%	71%	83%	64%	71%	59%	NA	0,59	578	579	240	239	0	407	0	364
Cropped Images	CovNet-UFCSPA	NA	75%	97%	91%	98%	83%	97%	80%	NA	0,798	792	745	25	72	0	244	0	527
	ResNet50 V2	NA	78%	80%	78%	89%	78%	80%	77%	NA	0,774	650	635	167	182	0	176	0	595
	Inception V3	NA	62%	81%	81%	89%	70%	81%	65%	NA	0,641	659	662	158	155	0	407	0	364

GCE Images	CovNet-UFCSPA	NA	70%	91%	84%	96%	77%	91%	74%	NA	0,732	747	687	70	130	0	290	0	481
	ResNet50 V2	NA	80%	89%	84%	94%	82%	89%	81%	NA	0,81	725	685	92	132	0	169	0	602
	Inception V3	NA	62%	83%	83%	90%	71%	83%	65%	NA	0,65	675	678	142	139	0	409	0	362
CLAHE Images	CovNet-UFCSPA	NA	56%	99%	96%	99%	70%	99%	59%	NA	0,574	808	781	9	36	0	623	0	148
	ResNet50 V2	NA	72%	94%	92%	97%	81%	94%	78%	NA	0,774	770	754	47	63	0	289	0	482
	Inception V3	NA	54%	90%	91%	95%	68%	90%	55%	NA	0,54	738	747	79	70	0	644	0	127
Mixed Images	CovNet-UFCSPA	NA	76%	NA	96%	NA	85%	NA	82%	NA	0,82	NA	781	NA	36	NA	242	NA	526
	ResNet50 V2	NA	81%	NA	92%	NA	86%	NA	85%	NA	0,848	NA	754	NA	63	NA	175	NA	593
	Inception V3	NA	65%	NA	91%	NA	76%	NA	70%	NA	0,692	NA	747	NA	70	NA	407	NA	361

Prec. - Precision/ NA - Not application / II - Experiment II / III - Experiment III

Conclusion

The CovNet-UFCSPA architecture's development involved several stages, from data handling to execution strategies, revealing early the need for robust hardware due to significant memory consumption during experiments. Key decisions like batch size directly depended on the available hardware resources. Initial tests were conducted on a machine equipped with 16 GB of RAM, an NVIDIA GeForce RTX 2060 GPU, and an Intel® Core™ i7 processor. However, this setup was inadequate for more complex models such as Resnet 50V2 and Inception V3, prompting a shift to the Santos Dumont environment which features more capable GPUs.

The architecture functioned smoothly at Santos Dumont without the need for distributed training techniques, except when dealing with models like Resnet50 V2 and Inception V3 with large batch sizes, where distributed training became necessary. Techniques such as ModelCheckpoint were employed to safeguard training progress against disruptions like memory overflows.

The architecture, tested primarily on COVID-19 patient data, faced a class imbalance, addressed by prioritizing recall and analyzing the confusion matrix. Preprocessing steps like cropping and CLAHE played crucial roles in enhancing model performance by minimizing false negatives. Comparative tests with the CovNet-UFCSPA model against established models verified the effectiveness of these techniques, particularly with data from Brazilian public hospital patients, showing accurate classifications but also revealing areas for improvement. Future strategies include expanding data types and ongoing training within Brazilian hospital networks to boost

diagnostic precision. Additionally, plans are underway to develop an online tool for immediate X-ray analysis to aid health professionals in preliminary screening alongside RT-PCR tests.

References

[1] Gong J, Dong H, Xia SQ, Huang YZ, Wang D, Zhao Y, Liu W, Tu S, Zhang M, Wang Q, et al. Correlation analysis between disease severity and inflammation-related parameters in patients with COVID-19 pneumonia. MedRxiv. 2020.

[2] Udugama B, Kadhiresan P, Kozlowski HN, Malekjahani A, Osborne M, Li VYC, Chen H, Mubareka S, Gubbay JB, Chan WCW. Diagnosing COVID-19: the disease and tools for detection. ACS Nano. 2020;14(4):3822-3835.

[3] DATASUS. Equipments of Imaging Used in Health - E - DATASUS. DATASUS. Available at: http://tabnet.datasus.gov.br/tabdata/LivroIDB/2edrev/e18.pdf

[4] Chassagnon G, Vakalopoulou M, Paragios N, Revel MP. Artificial intelligence applications for thoracic imaging. Eur J Radiol. 2020;123:108774.

[5] Nahid AA, Sikder N, Bairagi AK, Razzaque M, Masud M, Kouzani AZ, Mahmud MA, et al. A novel method to identify pneumonia through analyzing chest radiographs employing a multichannel convolutional neural network. Sensors. 2020;20(12):3482.

[6]Rajaraman S, Antani S. Training deep learning algorithms with weakly labeled pneumonia chest X-ray data for COVID-19 detection. medRxiv. 2020.

[7] Ozturk T, Talo M, Yildirim EA, Baloglu UB, Yildirim O, Acharya UR. Automated detection of COVID-19 cases using deep neural networks with X-ray images. Comput Biol Med. 2020;121:103792.

[8] Mittal A, Singh K, Misra DP. Detecting COVID-19 using ResNet deep learning model with X-ray images. Biocybernetics and Biomedical Engineering. 2020.

[9] Takara, K., Nishiyama, Y., & Sone, S. (2022). Artificial Intelligence System for Chest X-ray Diagnosis of COVID-19: Development and Validation Study. Journal of Medical Internet Research, 24(1), e30527.

[10] Nouara Cândida Xavier, Tathiane Alves Pianoschi Alva, Carla Diniz Lopes Becker. Ciências da Saúde: uma abordagem holística. Editora Conhecimento Livre; 2022. Cap 5.

[11] Gonzalez, Rafael C., and Richard E. Woods. Processamento de imagens digitais. Editora Blucher, 2000.

[13] Chollet F. Deep learning with Python. Simon and Schuster; 2021.

[14] Yamashita R, Nishio M, Do RK, Togashi K. Convolutional neural networks: an overview and application in radiology. Insights into Imaging. 2018;9(4):611-629.

[15] O'Shea K, Nash R. An introduction to convolutional neural networks. arXiv preprint arXiv:1511.08458. 2015.

[16] Albawi S, Mohammed TA, Al-Zawi S. Understanding of a convolutional neural network. In: 2017 International Conference on Engineering and Technology (ICET). IEEE; 2017. pp. 1-6.

[17] scikit. Sklearn.utils.class_weight.compute_class_weight. [Online]. Available in: https://scikit-learn.org/stable/modules/generated/sklearn.utils.class_weight.compute_class_weight.html. Access at: 2024.

[18] Cross-validation: evaluating estimator performance. [Online]. Available in: https://scikit-learn.org/stable/modules/cross_validation.html. Access at: 2024